

Sprinklers: A Randomized Variable-Size Striping Approach to Reordering-Free Load-Balanced Switching

WeiJun Ding^{*} Jim Xu[†] Jim Dai[‡] Yang Song[§] Bill Lin[¶]

June 7, 2014

Abstract

Internet traffic continues to grow exponentially, calling for switches that can scale well in both size and speed. While load-balanced switches can achieve such scalability, they suffer from a fundamental packet reordering problem. Existing proposals either suffer from poor worst-case packet delays or require sophisticated matching mechanisms. In this paper, we propose a new family of stable load-balanced switches called “Sprinklers” that has comparable implementation cost and performance as the baseline load-balanced switch, but yet can guarantee packet ordering. The main idea is to force all packets within the same virtual output queue (VOQ) to traverse the same “fat path” through the switch, so that packet reordering cannot occur. At the core of Sprinklers are two key innovations: a randomized way to determine the “fat path” for each VOQ, and a way to determine its “fatness” roughly in proportion to the rate of the VOQ. These innovations enable Sprinklers to achieve near-perfect load-balancing *under arbitrary admissible traffic*. Proving this property rigorously using novel worst-case large deviation techniques is another key contribution of this work.

1 Introduction

Internet service providers need high-performance switch architectures that can scale well in both size and speed, provide throughput guarantees, achieve low latency, and maintain packet ordering. However, conventional crossbar-based switch architectures with centralized scheduling and arbitrary per-packet dynamic switch configurations are not scalable.

An alternative class of switch architecture is the load-balanced switch, first introduced by Chang et al. [2, 3], and later further developed by others (e.g. [9, 11, 13]). These architectures rely on two switching stages for routing packets. Fig. 1 shows a diagram of a generic two-stage load-balanced switch. The first switch connects the first stage of input ports to the center stage of intermediate ports, and the second switch connects the center stage of intermediate ports to the final stage of

^{*}School of Industrial and Systems Engineering, Georgia Institute of Technology, wding34@gatech.edu

[†]College of Computing, Georgia Institute of Technology, jx@cc.gatech.edu

[‡]School of Operations Research and Information Engineering, Cornell University, Ithaca, NY 14853; on leave from Georgia Institute of Technology, jim.dai@cornell.edu

[§]Electrical and Computer Engineering, University of California, San Diego, y6song@eng.ucsd.edu

[¶]Electrical and Computer Engineering, University of California, San Diego, billlin@eng.ucsd.edu

output ports. Both switching stages execute a deterministic connection pattern such that each input to a switching stage is connected to each output of the switch at $1/N$ th of the time. This can be implemented for example using a deterministic round-robin switch (see Sec. 3.4). Alternatively, as shown in [11], the deterministic connection pattern can also be efficiently implemented using optics in which all inputs are connected to all outputs of a switching stage in parallel at a rate of $1/N$ th the line rate. This class of architectures appears to be a practical way to scale high-performance switches to very high capacities and line rates.

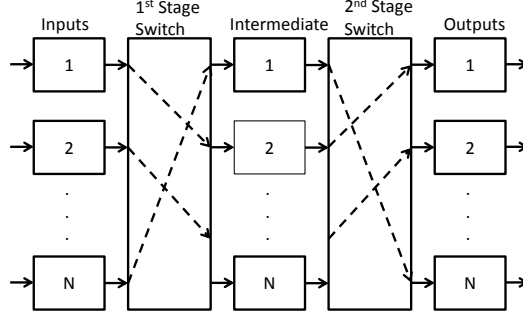


Figure 1: Generic load-balanced switch.

Although the baseline load-balanced switch originally proposed in [2] is capable of achieving throughput guarantees, it has the critical problem that packet departures can be badly out-of-order. In the baseline load-balanced switch, consecutive packets at an input port are spread to all N intermediate ports upon arrival. Packets going through different intermediate ports may encounter *different queueing delays*. Thus, some of these packets may arrive at their output ports out-of-order. This is detrimental to Internet traffic since the widely used TCP transport protocol falsely regards out-of-order packets as indications of congestion and packet loss. Therefore, a number of researchers have explored this packet ordering problem (e.g. [9, 11, 13]).

1.1 Our approach

In this paper, we propose “Sprinklers,” a new load-balanced switching solution that has comparable implementation cost and computational complexity, and similar performance guarantees as the baseline load-balanced switch, yet can guarantee packet ordering. The Sprinklers approach has a mild flavor of a simple, yet flawed solution called “TCP hashing”¹ [11]. The idea of TCP hashing is to force all packets at an input port that belong to the same application (TCP or UDP) flow to go through the same *randomly chosen* intermediate port by hashing on the packet’s flow identifier. This approach ensures that all packets that belong to the same application flow will depart the switch in order because they will encounter the *same queueing delay* through the same intermediate port. Although the TCP hashing scheme is simple and intuitive, it cannot guarantee stability because an intermediate port can easily be oversubscribed by having too many *large* flows randomly assigned to it.

Like the TCP hashing approach in which all packets within an application flow are forced to go through the same switching path, a Sprinklers switch requires all packets within a Virtual Output Queue (VOQ) to go down the *same* “fat path” called a stripe. Specifically, for each VOQ, a Sprinklers switch stripes packets within a VOQ across an interval of consecutive intermediate ports,

¹TCP hashing is referred to as “Application Flow Based Routing” (AFBR) in [11].

which we call a *stripe interval*. The number of intermediate ports L in the stripe interval is referred to as its *size*. In the Sprinklers approach, the size L of the stripe interval is determined roughly in proportion to the *rate* of the VOQ, and the placement of the L consecutive intermediate ports is by means of *random permutation*. Therefore, the N^2 stripe intervals, corresponding to the N^2 VOQs at the N input ports, can be very different from one another in both sizes and placements. The placement of variable-size stripes by means of random permutation ensures that the traffic loads associated with them get evenly distributed across the N intermediate ports.

For example, suppose a VOQ is assigned to the stripe interval $(8, 12]$ based on its arrival rate and random permutation, which corresponds to intermediate ports $\{9, 10, 11, 12\}$. Then the incoming packets belonging to this VOQ will be grouped in arrival order into stripes of $L = 4$ packets each. Once a stripe is filled, the $L = 4$ packets in the stripe will be transmitted to intermediate ports 9, 10, 11, and 12, respectively.

By making a stripe the basic unit of scheduling at both input and intermediate ports, a Sprinklers switch ensures that every stripe of packets departs from its input port and arrives at its output port both “in one burst” (i.e., in consecutive time slots). This “no interleaving between the servicing of two stripes” service guarantee, combined with the FCFS order in which packets within a stripe and stripes within a VOQ are served, ensures that packet reordering cannot happen within any VOQ, and hence cannot happen within any application flow either.

1.2 Contributions of the paper

This paper makes the following major contributions:

- First, we introduce the design of a new load-balanced switch architecture based on randomized and variable-size striping that we call Sprinklers. Sprinklers is indeed scalable in that all its algorithmic aspects can be implemented in constant time at each input port and intermediate port in a fully distributed manner.
- Second, we develop novel large deviation techniques to prove that Sprinklers is stable under intensive arrival rates with overwhelming probability, while guaranteeing packet order.
- Third, to our knowledge, Sprinklers is the first load-balanced switch architecture based on randomization that can guarantee both stability and packet ordering, which we hope will become the catalyst to a rich family of solutions based on the simple principles of randomization and variable stripe sizing.

1.3 Outline of the paper

The rest of the paper is organized as follows. Sec. 2 provides a brief review of existing load-balanced switch solutions. Sec. 3 introduces the structure of our switch and explains how it works. Sec. 4 provides a rigorous proof of stability based on the use of convex optimization theory and negative association theory to develop a Chernoff bound for the overload probability. This section also presents our worst-case large deviation results. Sec. 6 evaluates our proposed architecture, and Sec. 7 concludes the paper.

2 Existing Load-Balanced Switch Solutions

2.1 Hashing-Based

As discussed in Sec. 1, packets belonging to the same TCP flow can be guaranteed to depart from their output port in order if they are forced to go through the same intermediate port. The selection of intermediate port can be easily achieved by hashing on the packet header to obtain a value from 1 to N . Despite its simplicity, the main drawback of this TCP hashing approach is that stability cannot be guaranteed [11].

2.2 Aggregation-Based

An alternative class of algorithms to hashing is based on aggregation of packets into frames. One approach called Uniform Frame Spreading (UFS) [11] prevents reordering by requiring that each input first accumulates a full-frame of N packets, all going to the same output, before uniformly spreading the N packets to the N intermediate ports. Packets are accumulated in separate virtual output queues (VOQs) at each input for storing packets in accordance to their output. When a full-frame is available, the N packets are spread by placing one packet at each of the N intermediate ports. This ensures that the lengths of the queues of packets destined to the same output are the same at every intermediate port, which ensures every packet going to the same output experiences the same queuing delay independent of the path that it takes from input to output. Although it has been shown in [11] that UFS achieves 100% throughput for any admissible traffic pattern, the main drawback of UFS is that it suffers from long delays, $O(N^3)$ delay in the worst-case, due to the need to wait for a full-frame before transmission. The performance of UFS is particularly bad at light loads because slow packet arrivals lead to much longer accumulation times.

An alternative aggregation-based algorithm that avoids the need to wait for a full-frame is called Full Ordered Frames First (FOFF) [11]. As with UFS, FOFF maintains VOQs at each input. Whenever possible, FOFF will serve full-frames first. When there is no full-frame available, FOFF will serve the other queues in a round-robin manner. However, when incomplete frames are served, packets can arrive at the output out of order. It has been shown in [11] that the amount of reordering is always bounded by $O(N^2)$ with FOFF. Therefore, FOFF adds a reordering buffer of size $O(N^2)$ at each output to ensure that packets depart in order. It has been shown in [11] that FOFF achieves 100% throughput for any admissible traffic pattern, but the added reordering buffers lead to an $O(N^2)$ in packet delays.

Another aggregation-based algorithm called Padded Frames (PF) [9] was proposed to avoid the need to accumulate full-frames. Like FOFF, whenever possible, FOFF will serve full-frames first. When no full-frame is available, PF will search among its VOQ at each input to find the longest one. If the length of the longest queue exceeds some threshold T , PF will pad the frame with fake packets to create a full-frame. This full-frame of packets, including the fake packets, are uniformly spread across the N intermediate ports, just like UFS. It has been shown in [9] that PF achieves 100% throughput for any admissible traffic pattern, but its worst-case delay bound is still $O(N^3)$.

2.3 Matching-Based

Finally, packet ordering can be guaranteed in load-balanced switches via another approach called a Concurrent Matching Switch (CMS) [13]. Like hashing-based and aggregation-based load-balanced

switch designs, CMS is also a fully distributed solution. However, instead of bounding the amount of packet reordering through the switch, or requiring packet aggregation, a CMS enforces packet ordering throughout the switch by using a fully distributed load-balanced scheduling approach. Instead of load-balancing packets, a CMS load-balances request tokens among intermediate ports, where each intermediate port concurrently solves a local matching problem based only on its local token count. Then, each intermediate port independently selects a VOQ from each input to serve, such that the packets selected can traverse the two load-balanced switch stages without conflicts. Packets from selected VOQs depart in order from the inputs, through the intermediate ports, and finally through the outputs. Each intermediate port has N time slots to perform each matching, so the complexity of existing matching algorithms can be amortized by a factor of N .

3 Our scheme

Sprinklers has the same architecture as the baseline load-balanced switch (see Fig. 1), but it differs in the way that it routes and schedules packets for service at the input and intermediate ports. Also, Sprinklers have N VOQs at each input port. In this section, we first provide some intuition behind the Sprinklers approach, followed by how the Sprinklers switch operates, including the striping mechanism for routing packets through the switch and the companion stripe scheduling policy.

3.1 Intuition Behind the Sprinklers Approach

The Sprinklers approach is based on three techniques for balancing traffic evenly across all N intermediate ports: permutation, randomization, and variable-size striping. To provide some intuition as to why all three techniques are necessary, we use an analogy from which the name Sprinklers is derived. Consider the task of watering a lawn consisting of N identically sized areas using N sprinklers with different pressure. The objective is to distribute an (ideally) identical amount of water to each area. This corresponds to evenly distributing traffic inside the N VOQs (sprinklers) entering a certain input port to the N intermediate ports (lawn areas) under the above-mentioned constraint that all traffic inside a VOQ must go through the same set of intermediate ports (i.e., the stripe interval) to which the VOQ is mapped.

An intuitive and sensible first step is to aim exactly one sprinkler at each lawn area, since aiming more than one sprinklers at one lawn area clearly could lead to it being flooded. In other words, the “aiming function,” or “which sprinkler is aimed at which lawn area,” is essentially a permutation over the set $\{1, 2, \dots, N\}$. This permutation alone however cannot do the trick, because the water pressure (traffic rate) is different from one sprinkler to another, and the lawn area aimed at by a sprinkler with high water pressure will surely be flooded. To deal with such disparity in water pressures, we set the “spray angle range” of a sprinkler, which corresponds to the size (say L) of the stripe interval for the corresponding VOQ, proportional to its water pressure, and evenly distribute this water pressure across the L “streams” of water that go to the target lawn area and $L - 1$ “neighboring” lawn areas.

However, such water pressure equalization (i.e., variable stripe sizing) alone does not prevent all scenarios of load-imbalance because it shuffles water around only “locally.” For example, if a larger than average number of high pressure sprinklers are aimed at a cluster of lawn areas close to one another, some area within this cluster will be flooded. Hence, a simple yet powerful randomized

algorithm is brought in to shuffle water around globally: we simply sample this permutation at uniform random from the set of all $N!$ permutations.

Besides load-balancing, there is another important reason for the size of a stripe interval to be set roughly proportional to the traffic rate of the corresponding VOQ. In some existing solutions to the packet reordering problem with load-balanced switches, each VOQ has to accumulate a full frame of N packets before the frame can depart from the input port. For a VOQ with low traffic rate, this buffering delay could be painfully long. By adopting rate-proportional stripe sizing, a Sprinklers switch significantly reduces the buffering delays experienced by the low-rate VOQs.

As far as the Sprinklers analogy goes, the combination of randomized permutation and water pressure equalization, with proper “manifoldization” (i.e., considering $N + 1$ as 1), will provably ensure that the amount of water going to each lawn area is very even with high probability. However, because the servicing of any two stripes cannot interleave in a Sprinklers switch (to ensure correct packet order), two stripes have to be serviced in two different frames (N time slots), even if their stripe intervals overlap only slightly. A rampant occurrence of such slight overlaps, which can happen if the stripe interval size of a VOQ is set strictly proportional to the rate of the VOQ (rounded to an integer), will result in gross waste of service capacity, and significantly reduce the maximum achievable throughput.

Therefore, we would like any two stripe intervals to either “bear hug” (i.e., one contained entirely in the other) or does not touch (no overlap between the intervals) each other. Our solution is a classical “computer science” one: making N a power of 2 (very reasonable in the modern switching literature) and every stripe interval a dyadic one (resulting from dividing the whole interval $(0, N]$ into 2^k equal-sized subintervals for an integer $k \leq \log_2 N$). Now that the spray angle range of a sprinkler has to be a power of 2, the water pressure per stream could vary from one sprinkler to another by a maximum factor of 2. However, as shown later in Sec. 4, strong statistical load-balancing guarantees can still be rigorously proven despite such variations.

3.2 Operations of the Sprinklers Switch

As just explained, traffic inside each of the N^2 VOQs is switched through a dyadic interval of intermediate ports that is just large enough to bring the load imposed by the VOQ on any intermediate port within this interval (i.e., “water pressure per stream”) below a certain threshold. The sizes of the corresponding N^2 stripe intervals are determined by the respective rates of the corresponding VOQs, and their placements to consecutive intermediate ports are performed using a randomized algorithm. Once generated, their placements remain fixed thereafter, while their sizes could change when their respective rates do. Our goal in designing this randomized algorithm is that, when switched through the resulting (random) stripe intervals, traffic going out of any input port or going into any output port is near-perfectly balanced across all N intermediate ports, with overwhelming probabilities.

Once the N^2 stripe intervals are generated and fixed, packets in each VOQ will be striped across its corresponding interval of intermediate ports as follows. Fix an arbitrary VOQ, and let its stripe size and interval be 2^k and $(\ell, \ell + 2^k] \equiv \{\ell + 1, \ell + 2, \dots, \ell + 2^k\}$, respectively. (The integer ℓ must be divisible by 2^k for the interval to be dyadic, as discussed earlier.) Packets in this VOQ are divided, chronologically according to their arrival times, into groups of 2^k packets each and, with a slight abuse of the term, we refer to each such group also as a stripe. Such a stripe will eventually be switched through the set of intermediate ports $\{\ell + 1, \ell + 2, \dots, \ell + 2^k\}$ as follows. Assume

this switching operation starts at time (slot) t , when the corresponding input port is connected to the intermediate port $\ell + 1$ by the first switching fabric. Then, following the periodic connection sequence of the first switching fabric, the input port forwards the first packet in the stripe to the intermediate port $\ell + 1$ at time t , the second packet to the intermediate port $\ell + 2$ at time $t + 1$, and so on, until it forwards the last packet in the stripe to the intermediate port $\ell + 2^k$ at time $t + 2^k - 1$. That is, packets in this stripe go out of the input port to consecutive intermediate ports in consecutive time slots (i.e., “continuously”). The same can be said about other stripes from this and other VOQs. This way, at each input port, the (switching) service is rendered by the first switching fabric in a stripe-by-stripe manner (i.e., finish serving one stripe before starting to serve another).

At each input port, packets from the N VOQs originated from it compete for (the switching) service by the first switching fabric and hence must be arbitrated by a scheduler. However, since the service is rendered stripe-by-stripe, as explained above, the scheduling is really performed among the competing stripes. In general, two different scheduling policies are needed in a Sprinklers switch, one used at the input ports and the other at intermediate ports. Designing stripe scheduling policies that are well suited for a Sprinklers switch turns out to be a difficult undertaking because two tricky design requirements have to be met simultaneously.

The first requirement is that the resulting scheduling policies must facilitate a highly efficient utilization of the switching capacity of both switching fabrics. To see this, consider input port i , whose input link has a normalized rate of 1, and intermediate port ℓ . As explained in Sec. 1, these two ports are connected only once every N time slots, by the first switching fabric. Consider the set of packets at input port i that needs to be switched to the intermediate port ℓ . This set can be viewed and called a queue (a queueing-theoretic concept), because the stripe scheduling policy naturally induces a service order (and hence a service process) on this set of packets, and the arrival time of each packet is simply that of the stripe containing the packet. Clearly, the service rate of this queue is exactly $1/N$. Suppose this input port is heavily loaded say with a normalized arrival rate of 0.95. Then even with perfect load-balancing, the arrival rate to this queue is $0.95/N$, only slightly below the service rate $1/N$. Clearly, for this queue to be stable, there is no room for any waste of this service capacity. In other words, the scheduling policy must be throughput optimal.

The second requirement is exactly why we force all packets in a VOQ to go down the same fat path (i.e., stripe interval) through a Sprinklers switch, so as to guarantee that no packet reordering can happen. It is easy to verify that for packet order to be preserved within every stripe (and hence within every VOQ), it suffices to guarantee that packets in every stripe go into their destination output port from consecutive intermediate ports in consecutive time slots (i.e., continuously). However, it is much harder for a stripe of 2^k packets to arrive at an output port continuously (than to leave an input port), because these packets are physically located at a single input port when they leave the input port, but across 2^k different intermediate ports right before they leave for the output port.

After exploring the entire space of stripe-by-stripe scheduling policies, we ended up adopting the same stripe scheduling policy, namely Largest Stripe First (LSF), at both input ports and intermediate ports, but not for the same set of reasons. At input ports, LSF is used because it is throughput optimal. At intermediate ports, LSF is also used because it seems to be the only policy that makes every stripe of packets arrive at their destination output port continuously without incurring significant internal communication costs between the input and intermediate ports. In Sec. 3.4, we will describe the LSF policies at the input and intermediate ports.

3.3 Generating Stripe Intervals

As we have already explained, the random permutation and the variable dyadic stripe sizing techniques are used to generate the stripe intervals for the N VOQs originated from a single input port, with the objective of balancing the traffic coming out of this input port very evenly across all N intermediate ports. In Sec. 3.3.1, we will specify this interval generating process precisely and provide detailed rationales for it. In Sec. 3.3.2, we will explain why and how the interval generating processes at N input ports should be carefully coordinated.

3.3.1 Stripe interval generation at a single input port

Suppose we fix an input port and number the N VOQs originated from it as $1, 2, \dots, N$, respectively. VOQ i is first mapped to a distinct *primary intermediate port* $\sigma(i)$, where σ is a permutation chosen uniformly randomly from the set of all permutations on the set $\{1, 2, \dots, N\}$. Then the stripe interval for a VOQ i whose primary intermediate port is $\sigma(i)$ and whose interval size is n , which must be a power of 2 as explained earlier, is simply the unique dyadic interval of size n that contains $\sigma(i)$. A dyadic interval is one resulting from dividing the whole port number range $(0, N] \equiv \{1, 2, \dots, N\}$ evenly by a power of 2, which takes the form $(2^{k_0}m, 2^{k_0}(m+1)]$ where k_0 and m are nonnegative integers.

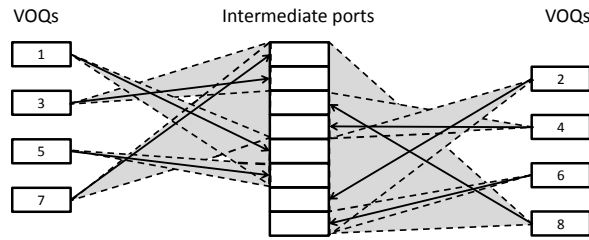


Figure 2: An example of VOQs being mapped to stripe intervals.

In Fig. 2, we show an example of mapping 8 VOQs at a single input port to their stripe intervals in an 8 by 8 switch. The middle column stands for the 8 intermediate ports and the columns on the left and on the right correspond to VOQs 1, 3, 5, 7 and VOQs 2, 4, 6, 8, respectively. Mapping a VOQ to its primary intermediate port is indicated by a solid arrow connecting the two. Its stripe interval is indicated by the “fanout” shadow that contains the solid line and is bounded at both ends by two dashed lines. For example, VOQ 7 (bottom one on the left) is mapped to the primary intermediate port 1 and its stripe size is 4. Therefore, its stripe interval is $(0, 4]$, the size-4 dyadic interval that contains intermediate port 1.

3.3.2 Stripe Size Determination

As mentioned in the “water pressure equalization” analogy, for a VOQ, the size of its stripe interval is roughly proportional to the (current) traffic rate of the VOQ. More precisely, the stripe interval size for a VOQ of traffic rate r , is determined by the following function:

$$F(r) = \min \left\{ N, 2^{\lceil \log_2(rN^2) \rceil} \right\}. \quad (1)$$

The stripe size determination rule (1) tries to bring the amount of traffic each intermediate port within the stripe interval receives from this VOQ below $1/N^2$ while requiring that the stripe size be a power of 2. However, if the rate r is very high, say $> \frac{1}{N}$, then the stripe size $F(r)$ is simply N .

The initial sizing of the N^2 stripe intervals may be set based on historical switch-wide traffic matrix information, or to some default values. Afterwards, the size of a stripe interval will be adjusted based on the measured rate of the corresponding VOQ. To prevent the size of a stripe from “thrashing” between 2^k and 2^{k+1} , we can delay the halving and doubling of the stripe size. Although our later mathematical derivations assume the perfect adherence to the above stripe size determination rule, the change in the provable load-balancing guarantees is in fact negligible when a small number of stripe sizes are a bit too small (or too large) for the respective rates of their corresponding VOQs.

3.3.3 Coordination among all N^2 stripe intervals

Like an input port, an output port is connected to each intermediate port also exactly once every N time slots, and hence needs to near-perfectly balance the traffic load coming into it. That is, roughly $\frac{1}{N}$ of that load should come from each intermediate port. In this section, we show how to achieve such load balancing at an output port, by a careful coordination among the (stripe-interval-generating) permutations σ_i , $i = 1, 2, \dots, N$.

Now consider an arbitrary output port j . There are precisely N VOQs destined for it, one originated from each input port. Intuitively, they should ideally be mapped (permuted) to N distinct primary intermediate ports – for the same reason why the N VOQs originated from an input port are mapped (permuted) to N distinct primary intermediate ports – by the permutations $\sigma_1, \sigma_2, \dots, \sigma_N$, respectively. We will show this property holds for every output port j if and only if the matrix representation of these permutations is an Orthogonal Latin Square (OLS).

Consider an $N \times N$ matrix $A = (a_{ij})$, $i, j = 1, 2, \dots, N$, where $a_{ij} = \sigma_i(j)$. Consider the N VOQs originated at input port i , one destined for each output port. We simply number each VOQ by its corresponding output port. Clearly row i of the matrix A is the primary intermediate ports of these N VOQs. Now consider the above-mentioned N VOQs destined for output port j , one originated from each input port. It is easy to see that the j th column of matrix A , namely $\sigma_1(j), \sigma_2(j), \dots, \sigma_N(j)$, is precisely the primary intermediate ports to which these N VOQs are mapped. As explained earlier, we would like these numbers also to be distinct, i.e., a permutation of the set $\{1, 2, \dots, N\}$. Therefore, every row or column of the matrix A must be a permutation of $\{1, 2, \dots, N\}$. Such a matrix is called an OLS in the combinatorics literature [4].

Our worst-case large deviation analysis in Sec. 4 requires the N VOQs at the same input port or destined to the same output port select their primary intermediate ports according to a uniform random permutation. Mathematically, we only require the marginal distribution of the permutation represented by each row or column of the OLS A to be uniform. The use of the word “marginal” here emphasizes that we do not assume any dependence structure, or the lack thereof, among the N random permutations represented by the N rows and among those represented by the N columns. We refer to such an OLS as being weakly uniform random, to distinguish it from an OLS sampled uniformly randomly from the space of all OLS’ over the alphabet set $\{1, 2, \dots, N\}$, which we refer to as being strongly uniform random. This distinction is extremely important for us, since whether there exists a polynomial time randomized algorithm for generating an OLS that is

approximately strongly uniform random has been an open problem in theoretical computer science and combinatorics for several decades [6, 8]. A weakly uniform random OLS, on the other hand, can be generated in $O(N \log N)$ time, shown as following.

We first generate two uniform random permutations $\sigma^{(R)}$ and $\sigma^{(C)}$ over the set $\{1, 2, \dots, N\}$ that are mutually independent, using a straightforward randomized algorithm [7]. This process, which involves generating $\log_2 N! = O(N \log N)$ random bits needed to “index” $\sigma^{(R)}$ and $\sigma^{(C)}$ each, has $O(N \log N)$ complexity in total. Then each matrix element $a(i, j)$ is simply set to $(\sigma^{(R)}(i) + \sigma^{(C)}(j) \bmod N) + 1$. It is not hard to verify that each row or column is a uniform random permutation.

3.4 Largest Stripe First Policy

In this section, we describe our stripe scheduling policy called Largest Stripe First (LSF), which is used at both input and intermediate ports of a Sprinklers switch. LSF can be implemented in a straightforward manner, at both input and intermediate ports, using $N(\log_2 N + 1)$ FIFO queues (a data structure concept). Using an $N \times (\log_2 N + 1)$ 2D-bitmap to indicate the status of each queue (0 for empty, 1 for nonempty), the switch can identify the rightmost bit set in each row of the bitmap in constant time, which is used by LSF to identify the largest stripe to serve at each port.

We first provide a brief description of the periodic sequences of connections executed at both switching fabrics shown in Fig. 1. The first switching fabric executes a periodic “increasing” sequence, that is, at any time slot t , each input port i is connected to the intermediate port $((i + t) \bmod N) + 1$. The second switching fabric, on the other hand, will execute a periodic “decreasing” sequence, that is, at any time slot t , each intermediate port ℓ is connected to the output port $((\ell - t) \bmod N) + 1$.

In the rest of the paper, we make the following standard homogeneity assumption about a Sprinklers switch. Every input, intermediate, or output port operates at the same speed. That is, each can process and transmit exactly one packet per time slot. We refer to this speed as 1. Every connection made in a switching fabric also has speed of 1 (i.e., one packet can be switched per time slot). Since N connections are made by a switching fabric at any time slot, up to N packets can be switched during the time slot.

3.4.1 Stripe Scheduling at Input Ports

Algorithm 1 LSF policy on “Who is next?”

```

1:  $l = (i + t \bmod N) + 1$ ;
2: if No stripe is being served at time  $t$  then
3:   Let  $S$  be the set of stripes with interval  $(l - 1, *]$ ;
4:   if  $S$  is not empty then
5:     Start serving the largest stripe in  $S$ ;
6:   end if
7: end if

```

The above pseudocode describes the Largest stripe first (LSF) policy used at input port i to make a decision as to, among multiple competing stripes, which one to serve next. Note that by the

stripe-by-stripe nature of the scheduler, it is asked to make such a policy decision only when it completely finishes serving a stripe. The policy is simply to pick among the set of stripes whose dyadic interval starts at intermediate port ℓ – provided that the set is nonempty – the largest one (FCFS for tie-breaking) to start serving immediately. The LSF policy is clearly throughput optimal because it is work-conserving in the sense whenever a connection is made between input port i and intermediate port ℓ , a packet will be served if there is at least one stripe at the input port whose interval contains ℓ . Using terms from queueing theory [12] we say this queue is served by a work-conserving server with service rate $1/N$.

A stripe service schedule, which is the outcome of a scheduling policy acting on the stripe arrival process, is represented by a schedule grid, as shown in Fig. 3. There are N rows in the grid, each corresponding to an intermediate port. Each tiny square in the column represents a time slot. The shade in the square represents a packet scheduled to be transmitted in that slot and different shade patterns mean different VOQs. Hence each “thin vertical bar” of squares with the same shade represents a stripe in the schedule. The time is progressing on the grid from right to left in the sense that packets put inside the rightmost column will be served in the first cycle (N time slots), the next column to the left in the second cycle, and so on. Within each column, time is progressing from up to down in the sense that packet put inside the uppermost cell will be switched to intermediate port 1 say at time slot t_0 , packet put inside the cell immediately below it will be switched to intermediate port 2 at time slot $t_0 + 1$, and so on. Note this up-down sequence is consistent with the above-mentioned periodic connection pattern between the input port and the intermediate ports. Therefore, the scheduler is “peeling” the grid from right to left and from up to down.

For example, Fig. 3 corresponds to the statuses of the scheduling grid at time t_0 and $t_0 + 8$, where LSF is the scheduling policy. We can see that the rightmost column in the left part of Fig. 3, representing a single stripe of size 8, is served by the first switching fabric in the meantime, and hence disappears in the right part of the figure. The above-mentioned working conservation nature of the LSF server for any input port is also clearly illustrated in Fig. 3: There is no “hole” in any row.

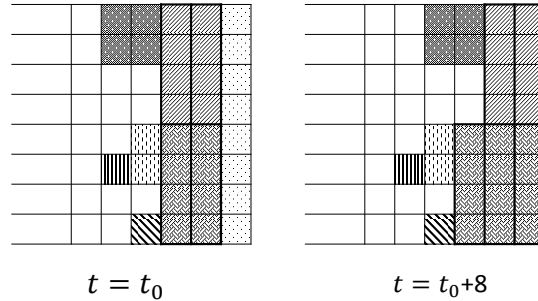


Figure 3: Statuses of the stripe scheduling at time t_0 (left) and $t_0 + 8$ (right) respectively.

While the scheduler always peels the grid from right to left and from up to down, the scheduler may insert a stripe ahead of other stripes smaller than it in size. In this case, the planned service time of all cells and bars to the left of the inserted vertical bar are shifted to the left by 1 column, meaning that their planned service time will be delayed by N time slots. For example, we can see from comparing the two parts of Fig. 3 that a stripe of size 4 is inserted in the lower part of the 3rd column in the right part of Fig. 3, after two other stripes of size 4, but before some other stripes of smaller sizes.

3.4.2 Implementation of LSF at an Input Port

In this section, we describe data structures and algorithms for implementing the Longest Stripe First scheduling policy at an input port. Again we use input port 1 as an illustrative example. The LSF policy at input port 1 can be implemented using $N(\log_2 N + 1)$ FIFO queues as shown in Fig. 4. Conceptually, these FIFO queues are arranged into an array with N rows and $\log_2 N + 1$ columns. Row ℓ corresponds to FIFO queues that buffer packets to be sent to intermediate port ℓ . Each column of FIFO queues is used to buffer stripes of a certain size. The last column is for stripes of size N , the second last for stripes of size $N/2$, and so on. The very first column is for stripes of size 1. Therefore, the FIFO on the ℓ th row and k th column is to queue packets going to intermediate port ℓ and from stripes of size 2^{k-1} .

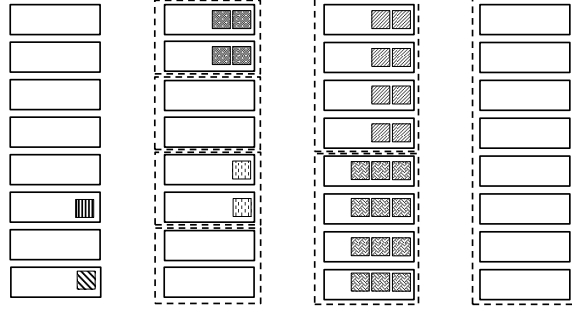


Figure 4: Data structure to implement LSF.

The implementation of LSF with this data structure is straightforward. Each VOQ will have a ready queue to buffer packets that have not filled up a stripe yet. Once a stripe is full, depending on the size of the stripe, it will be “plastered” into the corresponding interval in the corresponding column. At each column, stripes sent into the same interval will be queued in the FIFO order. For example, the contents of these FIFO queues at time $t_0 + 8$, that correspond to the scheduling grid shown as the right part of Fig. 3, are shown in Fig. 4.

During each time slot t , the scheduler either starts or is in the middle of serving the longest stripe that contain the intermediate port $t \bmod N$. However, the scheduler does not need to be stripe-aware. At each time t , it only needs to scan the $(t \bmod N)th$ row from right to left and serve the packet at the head of the first nonempty queue. If for each queue, we use a bit to encode whether it is empty, our problem boils down to looking for the “first one from right” in a bitmap $\log_2 N + 1$ bits long. This kind of operation can be done in one to a few clock cycles on modern processors or ASIC chip. Overall N such bitmaps are needed, one for each row (intermediate port).

Careful readers may note that it is unnecessary to maintain $N \log_2 N$ FIFO queues. Rather, we need only one FIFO queue for all stripes of size N , two for all stripes of size $N/2$, – namely one for the interval $(0, N/2]$ and the other for $(N/2, N]$, – four for all stripes of size $N/4$, and so on. The total number of FIFO queues we need is indeed $1 + 2 + 4 + \dots + N/2 + N = 2N - 1$. For example, in the above figure, we need only 15 queues: one FIFO queue for all stripes of size 8, two for all stripes of size 4, four for all stripes of size 2, and 8 for all stripes of size 1. We will indeed adopt such a simplified implementation for the input port. However, we still present the data structure in this “verbose” manner because this data structure will be modified for use at the intermediate ports, and there such a simplifying collapse is no longer possible, as will become clear next.

3.4.3 Stripe Scheduling at Intermediate Ports

In Sprinklers, an intermediate port also adopts the LSF policy for two reasons. First, throughput-optimality is needed also at an intermediate port for the same reason stated above. Second, given the distributed nature in which any scheduling policy at an intermediate port is implemented, LSF appears to be the easiest and least costly to implement.

The schedule grids at intermediate ports take a slightly different form. Every output port j is associated with a schedule grid also consisting of N rows. Row i of the grid corresponds to the tentative schedule in which packets destined for output port j at intermediate port i will follow. This schedule grid is really a virtual one, of which the N rows are physically distributed across N different intermediate ports respectively. All stripes heading to output j show up on this grid. The LSF policy can be defined with respect to this virtual grid in almost the same way as in the previous case.

The data structure for implementing LSF at intermediate ports is the same as that at input ports, except components of each instance are distributed across all N intermediate ports, thus requiring some coordination. This coordination however requires only that, for each packet switched over the first switching fabric, the input port inform the intermediate port of the size of the stripe to which the packet belongs. This information can be encoded in just $\log_2 \log_2 N$ bits, which is a tiny number (e.g., = 4 bits when $N = 4096$), and be included in the internal-use header of every packet transmitted across the first switching fabric.

4 Stability analysis

As explained in Sec. 3.4, a queueing process can be defined on the set of packets at input port i that need to be switched to intermediate port ℓ . This (single) queue is served by a work-conserving server with a service rate $1/N$ under the LSF scheduling policy. It has been shown in [5] that such a queue is stable as long as the long-term average arrival rate is less than $1/N$. This entire section is devoted to proving a single mathematical result, that is, the arrival rate to this queue is less than $1/N$ with overwhelming probability, under all admissible traffic workloads to the input port i .

Between input ports $i = 1, 2, \dots, N$ and intermediate ports $\ell = 1, 2, \dots, N$, there are altogether N^2 such queues to analyze. It is not hard to verify, however, that the joint probability distributions of the random variables involved in – and hence the results from – their analyses are identical. We will present only the case for $i = 1$ and $\ell = 1$. Thus, the queue in the rest of the section specifically refers to the one serving packets from input port 1 to intermediate port 1. With this understanding, we will drop subscripts i and ℓ in the sequel for notational convenience.

There are another N^2 queues to analyze, namely, the queues of packets that need to be transmitted from intermediate ports $\ell = 1, 2, \dots, N$ to output ports $j = 1, 2, \dots, N$. Note each such queue is also served by a work-conserving server with service rate $1/N$, because the LSF scheduling policy is also used at the intermediate ports, as explained in Sec. 3.4.3. Therefore, we again need only to prove that the arrival rate to each such queue is statistically less than $1/N$. However, again the joint probability distributions of the random variables involved in – and hence the results from – their analyses are identical to that of the N^2 queues between the input ports and the intermediate ports, this time due to the statistical rotational symmetry of the above-mentioned weakly random OLS based on which the stripe intervals are generated. Therefore, no separate analysis is necessary for these N^2 queues.

4.1 Formal statement of the result

In this section, we precisely state the mathematical result. Let the N VOQs at input port 1 be numbered $1, 2, \dots, N$. Let their arrival rates be r_1, r_2, \dots , and r_N , respectively, which we write also in the vector form \vec{r} . Let f_i be the stripe size of VOQ i , i.e., $f_i := F(r_i)$ for $i = 1, 2, \dots, N$, where $F(\cdot)$ is defined in Equation 1. Let s_i be the load-per-share of VOQ i , i.e., $s_i := \frac{r_i}{F(r_i)}$ for $i = 1, 2, \dots, N$. Let $|\vec{r}|$ be the sum of the arrival rates, i.e., $|\vec{r}| := r_1 + \dots + r_N$.

Let $X(\vec{r}, \sigma)$ be the total traffic arrival rate to the queue when the N input VOQs have arrival rates given by \vec{r} and the uniform random permutation used to map the N VOQs to their respective primary intermediate ports is σ . All N VOQs could contribute some traffic to this queue (of packets that need to be switched to intermediate port 1) and $X(\vec{r}, \sigma)$ is simply the sum of all these contributions. Clearly $X(\vec{r}, \sigma)$ is a random variable whose value depends on the VOQ rates \vec{r} and how σ shuffles these VOQs around.

Consider the VOQ that selects intermediate port ℓ as its primary intermediate port. By the definition of σ , the index of this VOQ is $\sigma^{-1}(\ell)$. It is not hard to verify that this VOQ contributes one of its load shares to this queue, in the amount of $s_{\sigma^{-1}(\ell)}$, if and only if its stripe size is at least ℓ . Denote this contribution as $X_\ell(\vec{r}, \sigma)$. we have $X_\ell(\vec{r}, \sigma) = s_{\sigma^{-1}(\ell)} \mathbb{1}_{\{f_{\sigma^{-1}(\ell)} \geq \ell\}}$. Then:

$$X(\vec{r}, \sigma) = \sum_{\ell=1}^N X_\ell(\vec{r}, \sigma). \quad (2)$$

Note all the randomness of $X_\ell(\vec{r}, \sigma)$ and hence $X(\vec{r}, \sigma)$ comes from σ , as \vec{r} is a set of constant parameters. The expectations of the functions of $X_\ell(\vec{r}, \sigma)$ and $X(\vec{r}, \sigma)$, such as their moment generating functions (MGF), are taken over σ . With this understanding, we will drop σ from $X_\ell(\vec{r}, \sigma)$ and $X(\vec{r}, \sigma)$ and simply write them as $X_\ell(\vec{r})$ and $X(\vec{r})$ in the sequel.

As explained earlier, the sole objective of this section is to prove that $\mathbb{P}(X(\vec{r}) \geq 1/N)$, the probability that the total arrival rate to this queue exceeds the service rate, is either 0 or extremely small. This probability, however, generally depends not only on $|\vec{r}|$, the total traffic load on input port 1, but also on how this total splits up (i.e., the actual rate vector \vec{r}).

Our result is composed of two theorems, namely, Theorems 1 and 2. Theorem 1 states that when this total load is no more than roughly $2/3$, then this probability is strictly 0, regardless of how it is split up. When the total traffic load $|\vec{r}|$ exceeds that amount, however, this probability could become positive, and how large this probability is could hinge heavily on the actual \vec{r} values. Theorem 2, together with the standard Chernoff bounding technique preceding it, provides a bound on the maximum value of this probability when the total load is no more than some constant ρ , but can be split up in arbitrary ways. More precisely, Theorem 2 helps establish an upper bound on $\sup_{\vec{r} \in V(\rho)} \mathbb{P}(X(\vec{r}) \geq 1/N)$, where $V(\rho) := \{\vec{r} \in \mathbb{R}_+^N : |\vec{r}| \leq \rho\}$. However, since $\mathbb{P}(X(\vec{r}) \geq 1/N)$, as a function of \vec{r} , is nondecreasing, this is equivalent to bounding $\sup_{\vec{r} \in U(\rho)} \mathbb{P}(X(\vec{r}) \geq 1/N)$, where $U(\rho) := \{\vec{r} \in \mathbb{R}_+^N : |\vec{r}| = \rho\}$. The same argument applies to $\mathbb{E}[\exp(\theta X(\vec{r}))]$, the MGF of $X(\vec{r})$. Therefore, we will use $U(\rho)$ instead of $V(\rho)$ in both cases in the sequel.

Theorem 1. $X(\vec{r}) < 1/N$ with probability 1 if $|\vec{r}| < \frac{2}{3} + \frac{1}{3N^2}$.

Let r_ℓ be the arrival rate of the VOQ that selects intermediate port ℓ as primary port. The corresponding stripe size and load-per-share of r_ℓ is given by f_ℓ and s_ℓ . Given the vector $\vec{r} =$

(r_1, \dots, r_N) , the arrival rate the queue (at input port 1, serving packets going to intermediate port 1) receives is $X(\vec{r}) = \sum_{\ell=1}^N s_\ell \mathbb{1}_{\{f_\ell \geq \ell\}}$. We prove Theorem 1 by studying the following problem.

$$\begin{aligned} \min_r : & \sum_{\ell=1}^N r_\ell \\ \text{s.t.} : & \sum_{\ell=1}^N s_\ell \mathbb{1}_{\{f_\ell \geq \ell\}} \geq 1/N \end{aligned} \quad (3)$$

Lemma 1. Suppose $r^* = (r_1^*, \dots, r_N^*)$ is an optimal solution to Problem (3). Then $f_\ell^* = 2^{\lceil \log_2 \ell \rceil}$ if $r_\ell^* > 0$, for $\ell = 1, \dots, N$.

Proof. We prove the lemma by contradiction.

1. Suppose there is $r_{\ell_0}^* > 0$ and $f_{\ell_0} < 2^{\lceil \log_2 \ell_0 \rceil}$, then $r_{\ell_0}^*$ does not contribute any arrival rate to the queue. Thus, we can reduce $r_{\ell_0}^*$ to zero without changing the total arrival rate to the queue. This contradicting the assumption that r^* is an optimal solution to Problem (3).
2. Suppose there is $r_{\ell_0}^* > 0$ and $f_{\ell_0}^* > 2^{\lceil \log_2 \ell_0 \rceil}$. According to stripe size rule (1), we know $s_{\ell_0}^* > 1/(2N^2)$.
 - (a) If $s_{\ell_0}^* \leq 1/N^2$, we construct solution $r' = r^*$ except we set $r'_{\ell_0} = 2^{\lceil \log_2 \ell_0 \rceil}/N^2$. $f_{\ell_0}^* > 2^{\lceil \log_2 \ell_0 \rceil}$ implies $f_{\ell_0}^* \geq 2 \times 2^{\lceil \log_2 \ell_0 \rceil}$. Further since $s_{\ell_0}^* > 1/(2N^2)$, we have that $r'_{\ell_0} < r_{\ell_0}^*$. It is easy to see that $X(r') > X(r^*)$, thus r' is also a feasible solution and has smaller total arrival rate than r^* . This contradicts the assumption that r^* is an optimal solution.
 - (b) If $s_{\ell_0}^* > 1/N^2$, implying $f_{\ell_0}^* = N$, we suppose $r_{\ell_0}^* = 1/N + N\varepsilon$. Since $N = f_{\ell_0}^* > 2^{\lceil \log_2 \ell_0 \rceil}$, we have $\ell_0 \leq N/2$. Construct $r' = r^*$ except set $r'_{\ell_0} = 2^{\lceil \log_2 \ell_0 \rceil}/2N^2 + \delta$ and $r'_{N/2+1} = r^*N/2 + 1 + (1/(2N^2) + \varepsilon)N$ where $0 < \delta \ll \varepsilon$. Then $X(r') = X(r^*) + \delta/2^{\lceil \log_2 \ell_0 \rceil} > X(r^*)$ and the total arrival rate of r' is smaller than that of r^* . This contradicts the assumption that r^* is an optimal solution.

To conclude, we establish the property in the lemma. \square

With the stripe size property in Lemma 1, if r^* is an optimal solution to Problem (3), then all r_1^* goes to the queue, $1/2$ of r_2^* goes to the queue, $1/4$ of r_3^* and r_4^* goes to the queue, and so on. To minimize the total arrival rate while have $X(r^*) \geq 1/N$, one should fill up r_ℓ^* that is closer to the queue first. Thus, $r_1^* = 1/N^2, r_2^* = 2/N^2, \dots, r_{N/4+1}^* = \dots = r_{N/2}^* = N/2 \cdot 1/N^2$. From these VOQs, the queue receives total arrival rate $N/2 \cdot 1/N^2 = 1/(2N)$. To achieve $X(r^*) = 1/N$, we set $r_{N/2+1}^* = N \cdot 1/(2N) = 1/2$ and all other $r_\ell^* = 0$. This optimal r^* results in total arrival rate $(1 + 2 + 4 + \dots + N/4 \cdot N/2)/N^2 + 1/2 = 2/3 + 1/(3N^2)$.

We now move on to describe the second theorem. By the standard Chernoff bounding technique, we have

$$\mathbb{P}(X(\vec{r}) \geq 1/N) \leq \inf_{\theta > 0} \exp(-\theta/N) \mathbb{E}[\exp(\theta X(\vec{r}))].$$

The above-mentioned worst-case probability can thus be upper-bounded as

$$\begin{aligned}
& \sup_{\vec{r} \in U(\rho)} \mathbb{P}(X(\vec{r}) \geq 1/N) \\
& \leq \sup_{\vec{r} \in U(\rho)} \inf_{\theta > 0} \exp(-\theta/N) \mathbb{E}[\exp(\theta X(\vec{r}))] \\
& \leq \inf_{\theta > 0} \sup_{\vec{r} \in U(\rho)} \exp(-\theta/N) \mathbb{E}[\exp(\theta X(\vec{r}))],
\end{aligned} \tag{4}$$

where the interchange of the infimum and supremum follows from the max-min inequality [1].

Therefore, our problem boils down to upper-bounding $\sup_{\vec{r} \in U(\rho)} \mathbb{E}[\exp(\theta X(\vec{r}))]$, the worst-case MGF of $X(\vec{r})$, which is established in the following theorem.

Theorem 2. When $\frac{2}{3} + \frac{1}{3N^2} \leq \rho < 1$, we have

$$\sup_{\vec{r} \in U(\rho)} \mathbb{E}[\exp(\theta X(\vec{r}))] \leq (h(p^*(\theta\alpha), \theta\alpha))^{N/2} \exp(\theta\rho/N),$$

where $h(p, a) = p \exp(a(1-p)) + (1-p) \exp(-ap)$, and

$$p^*(a) = \frac{\exp(a) - 1 - a}{\exp(a)a - a}$$

is the maximizer of $h(\cdot, a)$ for a given a .

For any given switch size N and a total load $\rho < 1$, Theorem 2 and the Chernoff bound (4) establish an upper bound on the above-mentioned worst-case probability. Table 1 provides the values of this probability under various settings of N and ρ . For example, when a Sprinklers switch has 2048 input and output ports (i.e., $N = 2048$) and is 93% loaded on input port 1, this upper bound is only 3.09×10^{-18} . Note however that it upper-bounds only the probability that a single queue, namely the set of packets at input port 1 that need to be switched to the intermediate ports 1, is overloaded. As mentioned earlier, there are altogether $2N^2$ such queues. Per the union bound, the probability that one or more such queues are overloaded across the entire 2048×2048 switch is simply $2N^2$ times that. In this example, the bound on the switch-wide overloading probability is 1.30×10^{-11} .

Table 1: Examples of overload probability bound

ρ	$N = 1024$	$N = 2048$	$N = 4096$
0.90	1.21×10^{-18}	1.14×10^{-29}	6.10×10^{-30}
0.91	3.06×10^{-15}	4.91×10^{-29}	7.10×10^{-30}
0.92	3.54×10^{-12}	1.26×10^{-23}	9.10×10^{-30}
0.93	1.76×10^{-9}	3.09×10^{-18}	1.58×10^{-29}
0.94	3.76×10^{-7}	1.42×10^{-13}	2.00×10^{-26}
0.95	3.50×10^{-5}	1.22×10^{-9}	1.48×10^{-18}
0.96	1.41×10^{-3}	1.99×10^{-6}	3.97×10^{-12}
0.97	2.50×10^{-2}	6.24×10^{-4}	3.90×10^{-7}

From these bounds, we can see that despite the use of the randomized and variable-size striping needed to prevent packet reordering and keeping the packet buffering delay within a reasonable range, a Sprinklers switch can achieve very high throughputs ($> 90\%$). In fact, the actual overloading probabilities could be orders of magnitude smaller, due to unavoidable relaxations used to

obtain such bounds. Another interesting phenomena reflected in Table 1 is that, given a traffic load, this bound decreases rapidly as the switch size N increases. In other words, the larger a Sprinklers switch is, the higher the throughput guarantees it can provide. This is certainly a desired property for a scalable switch.

4.2 Proof of Theorem 2

Recall $f_i = F(r_i)$ and $s_i = \frac{r_i}{f_i}$ for $i = 1, 2, \dots, N$. For the convenience of our later derivations, we rewrite X as a function of \vec{f} and \vec{s} by defining $X(\vec{s}, \vec{f}) = X(\vec{s} \circ \vec{f})$, where $\vec{s} \circ \vec{f} = (f_1 \cdot s_1, f_2 \cdot s_2, \dots, f_N \cdot s_N)$. With this rewriting, we can convert the optimization problem $\sup_{\vec{r} \in U(\rho)} \mathbb{E}[\exp(\theta X(\vec{r}))]$ in Theorem 2 to the following:

$$\sup_{\langle \vec{f}, \vec{s} \rangle \in A(\rho)} \mathbb{E}[\exp(\theta X(\vec{s}, \vec{f}))], \quad (5)$$

where

$$A(\rho) := \{ \langle \vec{f}, \vec{s} \rangle \mid f_\ell = 2^{k_\ell} \text{ for some integer } k_\ell, \forall \ell \quad (6)$$

$$s_\ell \in [0, \alpha] \text{ if } f_\ell = 1, \quad (7)$$

$$s_\ell \in (\alpha/2, \alpha] \text{ if } f_\ell = 2, 4, \dots, N/2 \quad (8)$$

$$s_\ell \in (\alpha/2, 1/N] \text{ if } f_\ell = N, \quad (9)$$

$$\sum_{\ell=1}^N s_\ell f_\ell = \rho \}. \quad (10)$$

The rule for stripe size determination (1) induces the conditions (6) - (9) above.

We now replace the half-open intervals in conditions (8) and (9) by the closed ones, which is equivalent to replacing $A(\rho)$ with its closure $\bar{A}(\rho)$, because it is generally much easier to work with a closed set in an optimization problem. The resulting optimization problem is

$$\max_{\langle \vec{f}, \vec{s} \rangle \in \bar{A}(\rho)} \mathbb{E}_\sigma[\exp(\theta X(\vec{s}, \vec{f}))]. \quad (11)$$

This replacement is logically correct because it will not decrease the optimal value of this optimization problem, and we are deriving an upper bound of it.

Our approach to Problem (11) is an exciting combination of convex optimization and the theory of negative associations in statistics [10], glued together by the Cauchy-Schwartz inequality. We first show that $\mathbb{E}[\exp(\theta X(\vec{s}, \vec{f}))]$, viewed as a function of only \vec{s} (i.e., with a fixed \vec{f}), achieves its maximum over $\bar{A}(\rho)$ when \vec{s} satisfies certain extremal conditions, through the convex optimization theory in Sec. 4.2.1. Then with \vec{s} fixed at any such extreme point, we can decompose $X(\vec{s}, \vec{f})$ into the sum of two sets of negatively associated (defined below) random variables. Using properties of negative association, we are able to derive a very tight upper bound on $\mathbb{E}[\exp(\theta X(\vec{s}, \vec{f}))]$ in Sec. 4.2.2.

Definition 1. Random variables X_1, X_2, \dots, X_k are said to be negatively associated if for every pair of disjoint subsets A_1, A_2 of $\{1, 2, \dots, k\}$,

$$\text{Cov}\{g_1(X_i, i \in A_1), g_2(X_j, j \in A_2)\} \leq 0,$$

whenever g_1 and g_2 are nondecreasing functions.

In the proof below, we need to use the following properties of negative association [10].

Lemma 2. *Let g_1, g_2, \dots, g_k be nondecreasing positive functions of one variable. Then X_1, \dots, X_k being negatively associated implies*

$$\mathbb{E} \left[\prod_{i=1}^k g_i(X_i) \right] \leq \prod_{i=1}^k \mathbb{E} [g_i(X_i)].$$

Lemma 3. *Let $x = (x_1, \dots, x_k)$ be a set of k real numbers. $X = (X_1, \dots, X_k)$ is a random vector, taking values in the set of $k!$ permutations of x with equal probabilities. Then $X = (X_1, \dots, X_k)$ is negatively associated.*

4.2.1 Extremal Property of \vec{s} in An Optimal Solution

Lemma 4. *Given $\frac{2}{3} + \frac{1}{3N^2} \leq \rho < 1$, for any $\theta > 0$, there is always an optimal solution $\langle \vec{f}^*, \vec{s}^* \rangle$ to Problem (11) that satisfies the following property:*

$$s_j^* = \begin{cases} 0 \text{ or } \alpha, & \text{if } f_j^* = 1; \\ \frac{\alpha}{2} \text{ or } \alpha, & \text{if } 2 \leq f_j^* \leq \frac{N}{2}. \end{cases} \quad (12)$$

Proof. Suppose $\langle \vec{f}^*, \vec{s}^* \rangle$ is an optimal solution to Problem (11). We claim that at least one scalar in \vec{f}^* is equal to N , since otherwise, the total arrival rate is at most $\frac{1}{N^2} \cdot \frac{N}{2} \cdot N = \frac{1}{2}$ by the stripe size determination rule (1), contradicting our assumption that $\rho \geq \frac{2}{3} + \frac{1}{3N^2} > \frac{1}{2}$. In addition, if more than one scalars in \vec{f}^* are equal to N , we add up the values of all these scalars in \vec{s} , assign the total to one of them (say s_m), and zero out the rest. This aggregation operation will not change the total arrival rate to any intermediate port because an input VOQ with stripe size equal to N will spread its traffic evenly to all the intermediate ports anyway.

If the optimal solution $\langle \vec{f}^*, \vec{s}^* \rangle$ does not satisfy Property (12), we show that we can find another optimal solution satisfying Property (12) through the following optimization problem. Note that now with \vec{f}^* fixed, $\mathbb{E}[\exp(\theta X(\vec{s}, \vec{f}^*))]$ is a function of only \vec{s} .

$$\max_{\vec{s}} : \mathbb{E}[\exp(\theta X(\vec{s}, \vec{f}^*))] \quad (13)$$

$$\text{s.t.} : 0 \leq s_j \leq \alpha, \forall j \text{ with } f_j^* = 1; \quad (14)$$

$$\frac{\alpha}{2} \leq s_j \leq \alpha, \forall j \text{ with } 2 \leq f_j^* \leq N/2; \quad (15)$$

$$\alpha/2 \leq s_m; \quad (16)$$

$$\sum_j s_j f_j^* = \rho. \quad (17)$$

$\mathbb{E}[\exp(\theta X(\vec{s}, \vec{f}^*))] = \frac{1}{N!} \sum_{\sigma} \exp\left(\theta \sum_{j=1}^N s_j \mathbb{1}_{\{f_j^* \geq \sigma(j)\}}\right)$ where $\sigma(j)$ is the index of the intermediate port that VOQ j is mapped to. Given \vec{f}^* , the objective function $\mathbb{E}[\exp(\theta X(\vec{s}, \vec{f}^*))]$ is clearly a convex function of \vec{s} .

The feasible region of \vec{s} defined by (14) - (17) is a (convex) polytope. By the convex optimization theory [1], the (convex) objective function reaches its optimum at one of the extreme points of

the polytope. The assumption $\rho \geq \frac{2}{3} + \frac{1}{3N^2}$ implies that Constraint (16) cannot be satisfied with equality. Thus, for any extreme point of the polytope, each of Constraint (14) and (15) must be satisfied with equality on one side. Thus there exists at least one optimal solution satisfying Property (12). This establishes the required result. \square

4.2.2 Exploiting Negative Associations

Suppose the optimization objective $\mathbb{E}[\exp(\theta X(\vec{s}, \vec{f}))]$ is maximized at \vec{s}^* , an extreme point of the above-mentioned polytope, and \vec{f}^* . In this section, we prove that $\mathbb{E}[\exp(\theta X(\vec{s}^*, \vec{f}^*))]$ is upper-bounded by the right-hand side (RHS) of the inequality in Theorem 2, by exploiting the negative associations – induced by \vec{s}^* being an extreme point – among the random variables that add up to $X(\vec{s}^*, \vec{f}^*)$. For notational convenience, we drop the asterisk from \vec{s}^* and \vec{f}^* , and simply write them as \vec{s} and \vec{f} .

Again for notational convenience, we further drop the terms \vec{f} and \vec{s} from $X(\vec{s}, \vec{f})$, and simply write it as X . Such a dependency should be clear from the context. We now split X into two random variables X^L and X^U and a constant X^d , by splitting each s_ℓ into s_ℓ^L and s_ℓ^U , and each f_ℓ into f_ℓ^L and f_ℓ^U , as follows. If $f_\ell = N$, we let $s_\ell^L = s_\ell^U = 0$. Otherwise, we define $s_\ell^L = \min\{s_\ell, \alpha/2\}$ and $s_\ell^U = \max\{0, s_\ell - \alpha/2\}$. We then define $f_\ell^L = f_\ell \mathbb{1}_{\{s_\ell^L = \alpha/2\}}$ and $f_\ell^U = f_\ell \mathbb{1}_{\{s_\ell^U = \alpha/2\}}$. It is not hard to verify that $s_\ell^L + s_\ell^U = s_\ell$ and $f_\ell^L + f_\ell^U = f_\ell$, for $\forall \ell$ if $f_\ell \leq N/2$. We further define $X^L = \sum_{\ell=1}^N \alpha/2 \cdot \mathbb{1}_{\{f_{\sigma^{-1}(\ell)}^L \geq \ell\}}$ and $X^U = \sum_{\ell=1}^N \alpha/2 \cdot \mathbb{1}_{\{f_{\sigma^{-1}(\ell)}^U \geq \ell\}}$. Finally, we define $X^d = \sum_{\ell=1}^N s_\ell \mathbb{1}_{\{f_\ell = N\}}$. X^d is the total arrival rate from the (high-rate) VOQs that have stripe size N , which is a constant because how much traffic any of these VOQs sends to the queue is not affected by which primary intermediate port σ maps the VOQ to. It is not hard to verify that $X = X^d + X^U + X^L$.

By the Cauchy-Schwartz inequality, we have

$$\begin{aligned} \mathbb{E}[\exp(\theta X(\vec{r}))] &= \exp(\theta X^d(\vec{r})) \mathbb{E}[\exp(\theta X^U(\vec{r})) \exp(\theta X^L(\vec{r}))] \\ &\leq \exp(\theta X^d(\vec{r})) (\mathbb{E}[\exp(2\theta X^L(\vec{r}))])^{1/2} \\ &\quad \cdot (\mathbb{E}[\exp(2\theta X^U(\vec{r}))])^{1/2}. \end{aligned} \tag{18}$$

Let $p_\ell^L = \mathbb{P}(f_{\sigma^{-1}(\ell)}^L \geq \ell)$. We now upper bound the MGF of X^L as follows:

$$\begin{aligned} \mathbb{E}[\exp(2\theta X^L)] &= \mathbb{E} \left[\exp \left(2\theta \cdot \alpha/2 \cdot \sum_{\ell=1}^N \mathbb{1}_{\{f_{\sigma^{-1}(\ell)}^L \geq \ell\}} \right) \right] \\ &= \mathbb{E} \left[\prod_{\ell=1}^N \exp \left(\theta \alpha \mathbb{1}_{\{f_{\sigma^{-1}(\ell)}^L \geq \ell\}} \right) \right] \\ &\leq \prod_{\ell=1}^N \mathbb{E} \left[\exp \left(\theta \alpha \mathbb{1}_{\{f_{\sigma^{-1}(\ell)}^L \geq \ell\}} \right) \right] \\ &= \prod_{\ell=1}^{N/2} \mathbb{E} \left[\exp \left(\theta \alpha \mathbb{1}_{\{f_{\sigma^{-1}(\ell)}^L \geq \ell\}} \right) \right] \\ &\leq \prod_{\ell=1}^{N/2} h(p^*(\theta \alpha), \theta \alpha) \exp(\theta \alpha p_\ell^L) \end{aligned}$$

$$= (h(p^*(\theta\alpha), \theta\alpha))^{N/2} \prod_{\ell=1}^{N/2} \exp(\theta\alpha p_\ell^L). \quad (19)$$

The first inequality holds due to Lemma 2 and the following two facts. First, $\{f_{\sigma^{-1}(1)}^L, f_{\sigma^{-1}(2)}^L, \dots, f_{\sigma^{-1}(N)}^L\}$, as a uniform random permutation of $\{f_1^L, f_2^L, \dots, f_N^L\}$, are negatively associated according to Lemma 3. Second, $\exp(\theta\alpha \mathbb{1}_{\{x \geq \ell\}})$ is a nondecreasing function of x for any given ℓ when $\theta > 0$. The third equality holds because with the way we define f^L above, $f_{\sigma^{-1}(\ell)}^L \leq N/2$ for any ℓ . The last inequality holds because each term in the product on the left-hand side, $\mathbb{E}[\exp(\theta\alpha \mathbb{1}_{\{f_{\sigma^{-1}(\ell)}^L \geq \ell\}})]$, is upper bounded by the corresponding term in the product on the RHS, $h(p^*(\theta\alpha), \theta\alpha) \exp(\theta\alpha p_\ell^L)$. It is not hard to verify because each $\mathbb{E}[\exp(\theta\alpha \mathbb{1}_{\{f_{\sigma^{-1}(\ell)}^L \geq \ell\}})]$ is the MGF of a Bernoulli random variable scaled by a constant factor $\theta\alpha$, and the function h reaches its maximum at p^* as defined in Theorem 2.

Letting $p_\ell^U = \mathbb{P}(f_{\sigma^{-1}(\ell)}^U \geq \ell)$, we can similarly bound $\mathbb{E}[\exp(2\theta X^U)]$ as follows:

$$\mathbb{E}[\exp(2\theta X^U)] \leq (h(p^*(\theta\alpha), \theta\alpha))^{N/2} \prod_{\ell=1}^{N/2} \exp(\theta\alpha p_\ell^U). \quad (20)$$

Combining (18), (19), and (20), we obtain

$$\begin{aligned} \mathbb{E}[\exp(\theta X)] &\leq (h(p^*(\theta\alpha), \theta\alpha))^{N/2} \\ &\quad \exp\left(\theta\left(X^d + \frac{\alpha}{2} \sum_{\ell=1}^{N/2} (p_\ell^L + p_\ell^U)\right)\right) \\ &= (h(p^*(\theta\alpha), \theta\alpha))^{N/2} \exp(\theta\rho/N). \end{aligned}$$

The final equality holds since $\rho/N = \mathbb{E}[X] = \mathbb{E}[X^d + X^L + X^U] = X^d + \frac{\alpha}{2} \sum_{\ell=1}^{N/2} (p_\ell^L + p_\ell^U)$. This concludes the proof of the theorem.

5 Expected delay at intermediate stage

In this section, we analyze the expected queue length at the intermediate ports. We are interested in this metric for two reasons. First, the queue length at these stations contribute to the total delay of the packets in this switch. Secondly and more importantly, when the switch detects changes of arrival rates to the input VOQs, the frame sizes of the input VOQs need to be redesigned. Before the packets with the new frame sizes are spread to the intermediate ports, the switch needs to make sure that the packets of previous frame sizes are all cleared. Otherwise, there could be reordering of the packets. The expected duration of this clearance phase is the average queue length at the stations.

We assume that the arrivals in different periods are identical and independently distributed. For a queuing system, given that the arrival rate is smaller than the service rate, the queue is stable and the queue length is mainly due to the burstiness of the arrivals. To make the arrivals have the maximum burstiness, we assume the arrival in each cycle (N time slots) is a Bernoulli random

variable that takes value N with probability $\frac{\rho}{N}$ and 0 with probability $1 - \frac{\rho}{N}$. We can construct a discrete time Markov process for the queue length *at the end of each cycle*. Its state space is $\{0, 1, \dots, \}$ and the nonzero transition probabilities are $\mathbb{P}_{i,i+N-1} = 1 - \frac{\rho}{N}$ for $i \geq 0$ and $\mathbb{P}_{i,i-1} = \frac{\rho}{N}$ for $i \geq 1$, and $\mathbb{P}_{0,0} = \frac{\rho}{N}$.

Given the transition matrix, we can solve for the stationary distribution, from which we can obtain the expected queue length. As figure 5 shows, the average delay in units of period is linear in the switch size. Given that our delay is analyzed against the worst burstiness and one cycle is at the magnitude of millisecond, this delay is very acceptable.

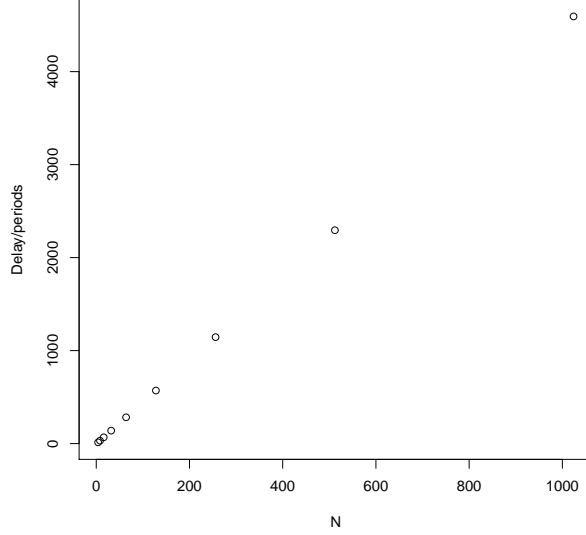


Figure 5: Expected delay when $\rho = 0.9$

6 Simulation

In this section, we present the simulation results of our switching algorithm and other existing switching algorithms under different traffic scenarios. The switching algorithms studied in this section include the baseline load-balanced switch [2], the uniform frame spreading (UFS) switch [11], the full-ordered frame first (FOFF) switch [11], and the padded frame (PF) switch [9]. The baseline load-balanced switch does not guarantee packet ordering, but it provides the lower bound of the average delay that a load-balanced switch can achieve. UFS, FOFF, and PF are known to provide reasonably good performance and all of them guarantee packet ordering.

In our simulation experiments, we assume a Bernoulli arrival to each input port, i.e. in each time slot, there is a packet arrival with probability ρ . The ρ parameter will be varied to study the performance of the switches under different loads. We also use different ways to determine the output port of each arrival packet. The size of the switch in the simulation study is $N = 32$.

Our first set of experiments assume uniform distribution of the destination port for the arrival packets, i.e. a new packet goes to output j with probability $\frac{1}{N}$. The simulation results are as shown in Fig. 6. The second set of experiments assume a diagonal distribution. A new packet

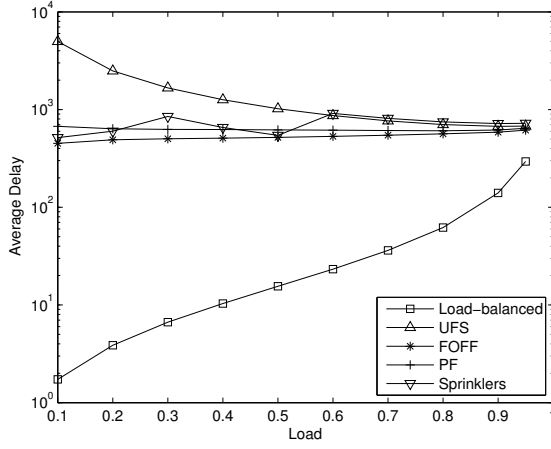


Figure 6: Average delay under uniform traffic

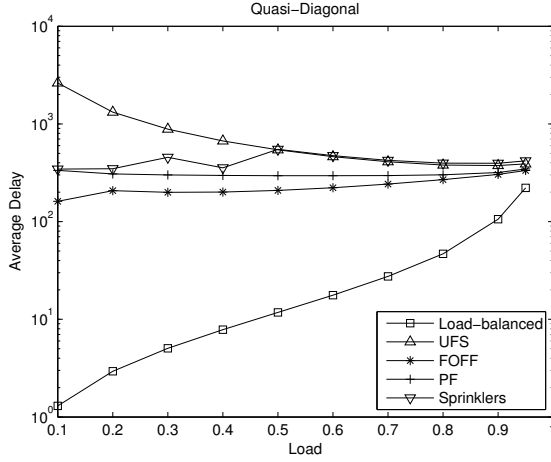


Figure 7: Average delay under diagonal traffic

arriving at input port i goes to output $j = i$ with probability $\frac{1}{2}$, and goes to any other output port with probability $\frac{1}{2(N-1)}$. The results are as shown in Fig. 7.

Our first observation of the comparison is that, under both the uniform and the diagonal traffic patterns, compared to UFS, our switch significantly reduces the average delay when the traffic load is low. This is understandable because the switch does not need to wait for additional packet to form a full frame. Secondly, like PF and FOFF, the average delay of our switching algorithm is quite stable under different traffic intensities. This property is quite preferable in practice. Finally, our switch has similar delay performance with PF and FOFF while the implementation of our switch is simpler than the other two switches.

7 Conclusion

In this paper, we proposed Sprinklers, a simple load-balanced switch architecture based on the combination of randomization and variable-size striping. Sprinklers has comparable implementation cost and performance as the baseline load-balanced switch, but yet can guarantee packet ordering.

We rigorously proved using worst-case large deviation techniques that Sprinklers can achieve near-perfect load-balancing under arbitrary admissible traffic. Finally, we believe that this work will serve as a catalyst to a rich family of solutions based on the simple principles of randomization and variable-size striping.

References

- [1] Stephen P Boyd and Lieven Vandenberghe. *Convex optimization*. Cambridge university press, 2004.
- [2] Cheng-Shang Chang, Duan-Shin Lee, and Yi-Shean Jou. Load balanced birkhoff–von neumann switches, part i: one-stage buffering. *Computer Communications*, 25(6):611–622, 2002.
- [3] Cheng-Shang Chang, Duan-Shin Lee, and Ching-Ming Lien. Load balanced birkhoff–von neumann switches, part ii: multi-stage buffering. *Computer Communications*, 25(6):623–634, 2002.
- [4] Charles J Colbourn. *CRC handbook of combinatorial designs*. CRC press, 1996.
- [5] JG Dai and Balaji Prabhakar. The throughput of data switches with and without speedup. In *INFOCOM 2000. Nineteenth Annual Joint Conference of the IEEE Computer and Communications Societies. Proceedings. IEEE*, volume 2, pages 556–564. IEEE, 2000.
- [6] Andy L Drizen. Generating uniformly distributed random 2-designs with block size 3. *Journal of Combinatorial Designs*, 20(8):368–380, 2012.
- [7] Richard Durstenfeld. Algorithm 235: random permutation. *Communications of the ACM*, 7(7):420, 1964.
- [8] Mark T Jacobson and Peter Matthews. Generating uniformly distributed random latin squares. *Journal of Combinatorial Designs*, 4(6):405–437, 1996.
- [9] Juan José Jaramillo, Fabio Milan, and R Srikant. Padded frames: a novel algorithm for stable scheduling in load-balanced switches. *Networking, IEEE/ACM Transactions on Networking*, 16(5):1212–1225, 2008.
- [10] Kumar Joag-Dev and Frank Proschan. Negative association of random variables with applications. *The Annals of Statistics*, 11(1):286–295, 1983.
- [11] Isaac Keslassy. *The load-balanced router*. PhD thesis, Stanford University, 2004.
- [12] Leonard Kleinrock. *Queueing systems. volume 1: Theory*. 1975.
- [13] Bill Lin and Isaac Keslassy. The concurrent matching switch architecture. *Networking, IEEE/ACM Transactions on*, 18(4):1330–1343, 2010.